Multiplication of electronic excitations in CaO and $YAlO_3$ crystals with free and self-trapped excitons

1994 J. Phys.: Condens. Matter 6 11177

(http://iopscience.iop.org/0953-8984/6/50/025)

J. Phys.: Condens. Matter 6 (1994) 11177–11187. Printed in the UK

Multiplication of electronic excitations in CaO and $YAlO_3$ crystals with free and self-trapped excitons

Ch Lushchik†, E Feldbach†, A Frorip†, M Kirm‡, A Lushchik†, A Maaroos† and I Martinson‡

† Institute of Physics, Estonian Academy of Sciences, Riia 142, EE-2400 Tartu, Estonia
‡ Department of Atomic Spectroscopy, Lund University, Sölvegatan 14 S-22362 Lund, Sweden

Received 18 July 1994

Abstract. Using synchrotron radiation of 6–32 eV the reflection spectrum and excitation spectra for 5.7, 4.6 and 2.8 eV emissions have been measured for a freshly cleaved CaO crystal at LHeT. In CaO, indirect band-to-band transitions take place in the region of $h\nu \geqslant 6.4$ eV. The excitation spectra for intrinsic emissions of 5.9 and 4.2 eV were measured in a $YAlO_3$ crystal at LHeT as well. As in many other dielectrics the electron–hole mechanism of multiplication of electronic excitations connected with the creation of secondary electron–hole pairs by hot photoelectrons also occurs in CaO and $YAlO_3$ crystals. The creation of secondary excitons by hot photoelectrons has been detected in $YAlO_3$ for the first time. The excitonic mechanism of multiplication of electronic excitations has a high efficiency in crystals with self-trapping excitons of small radii.

1. Introduction

After the development of growth methods of high-purity MgO and CaO crystals [1, 2] and the first measurements of optical and EPR characteristics of these crystals [2, 3] the electronic structure of wide-gap metal oxides has been thoroughly investigated by means of optical methods. Metal oxides with an energy gap $E_g > 5$ eV can be divided into two groups [4]. For the first group of crystals with cubic structure (e.g. MgO), narrow absorption bands at the edge of fundamental absorption [3] as well as resonant emission bands [5] have been observed. These bands arise from the formation and radiative decay of free excitons (FEs) with the radii significantly exceeding interionic distances. For the second group of oxides with lower symmetry (e.g. Y_2O_3 and Al_2O_3), broad exciton bands at the edge of intrinsic absorption and also luminescence of self-trapped excitons (STs) with large Stokes shifts have been revealed [6–8].

The use of synchrotron radiation (SR) has made it possible to investigate the effect of multiplication of electronic excitations (MEE) in a wide spectral region (up to 30–40 eV) for MgO and Y_2O_3 crystals [9–12]. However, the peculiarities of MEE processes in wide-gap oxides with FEs and STEs have not been analysed yet. The aim of the present study is partly to fill this gap by comparing MEE processes in a CaO crystal with large-radius FEs and in a $YAlO_3$ crystal with STEs, the effective radii of which are comparable with interionic distances. We have assumed that, similar to MgO [9], the main MEE mechanism in CaO is connected with the formation of secondary electron–hole pairs by hot photoelectrons. In a $YAlO_3$ crystal, it is expected that, in addition to this electron–hole mechanism, the realization of the excitonic MEE mechanism occurs owing to the creation of secondary excitons with

0953-8984/94/5011177+11$19.50

small radii by hot photoelectrons (similar to Y_2O_3 [10, 11]). Our experimental results have confirmed these hypotheses.

2. Experimental details

A single crystal of CaO was grown by the arc-fusion method from high-purity $CaCO_3$ at the Institute of Physics, Tartu [13]. In order to obtain a fresh surface the crystal was cleaved at LHeT in a vacuum of about 10^{-9} Torr by a specially designed mechanical cleaving system. The optical characteristics of CaO crystals were investigated in [3, 14, 15] and those of the samples used in the present study in [16, 17]. A $YAlO_3$ crystal was grown by the Czochralski method. The optical characteristics of $YAlO_3$ have been investigated and were detailed in [7, 18], while luminescence spectra and one- and two-photon absorption spectra were reported in [19, 20].

The present experiments were carried out at beamline 52 in the MAX-Laboratory in Lund (550 MeV storage ring). The experimental set-up has been briefly described in [21, 22]. SR is focused on the entrance slit of a 1 m normal-incidence vacuum monochromator with a gold-coated 1200 lines mm^{-1} grating (dispersion, 0.8 nm mm^{-1}). The samples were placed in a cold-finger helium cryostat evacuated with a turbomolecular pump (the lowest temperature is about 8 K, which will be called LHeT in this paper). The spectral distribution of the incident SR was taken into account by means of a two-channel photon-counting system. The emission from the sample was analysed in the 2–6 eV region using a MDR-12 monochromator (dispersion, 2.4 nm mm^{-1}; aperture, 1:3). The reference signal for normalization was recorded from a sodium-salicylate-coated mesh. Excitation spectra were measured at equal quantum intensities of the excitation falling onto the crystal.

3. Experimental results

3.1. Reflection spectra of a CaO crystal

The reflection spectrum of CaO has been previously measured at room temperature in a wide spectral region, up to 35 eV, using incident radiation of a hydrogen glow discharge or a pulsed argon-spark discharge source [3]. Similar data exist for the region 6–8 eV at 80 and 25 K [14]. For these measurements, highly hygroscopic CaO crystals were cleaved in a dry nitrogen atmosphere and then placed in a cryostat. The reflection spectrum of a CaO crystal has also been measured at 77 K using SR [15].

In our experiments a CaO crystal, freshly cleaved in air, was mounted without delay in a cryostat and, after evacuation for a few hours, the reflection spectrum was recorded at LHeT. As seen in figure 1 (full squares), the crystal surface became contaminated during the mounting and evacuation of the cryostat, and the spectrum shows no structure. Therefore a specially designed mechanical system was used for the additional cleavage of the crystal at LHeT under high-vacuum conditions. The reflection spectrum for the (100) plane of the CaO crystal was measured at an incidence angle of 45° immediately after the additional cleavage (figure 1; see also figure 3(a) later). The reflection spectrum of the crystal surface remained almost unchanged after excitation by SR at LHeT during several hours.

Figure 1 presents the short-wavelength part of this reflection spectrum measured at LHeT (about 4 meV resolution at 7 eV). There is a broad maximum at 6.85 eV (half-width, about 0.35 eV) and a number of narrow peaks at 6.943, 6.946, 6.979, 7.01, 7.036, 7.046, 7.093 and 7.105 eV. The positions of the narrow peaks are determined after computer analysis

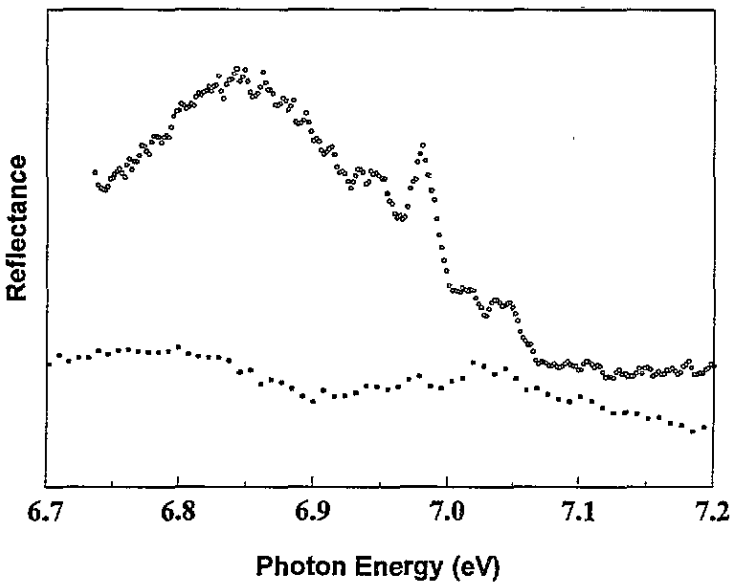

Figure 1. The reflecting spectrum of a CaO crystal measured at 8 K (spectral resolution, 0.08 nm) before (■) and immediately after (○) cleavage of the crystal at LHeT in high vacuum.

with an accuracy of ±2 meV. In [14], two doublets at 6.939, 6.973 eV and 7.012, 7.034 eV were observed in the reflection spectrum of CaO at 25 K. The peaks at 6.939 and 6.973 eV were interpreted as the formation of sin–orbit split $n = 1$ excitons with a large radius at the Γ point of the Brillouin zone. In contrast, the structure of our reflection spectrum is more complicated. The understanding of this structure needs special theoretical analysis which will be presented in a forthcoming paper.

3.2. Luminescence of a CaO crystal

Irradiation of a CaO crystal, cleaved at LHeT, by 21.5 eV photons results in the excitation of broad luminescence bands with the maxima at 5.7, 4.63 and 2.8 eV. It has been supposed in [23] that the 5.7 eV band corresponds to the emission of STEs. However, the intensity of this emission band depends linearly on the concentration of Mg^{2+} impurity ions, which are present in almost all CaO crystals. The Mg^{+} ions have been detected by the EPR method in irradiated CaO:Mg crystals [24]. The ionization potential of a free Mg^{+} ion is 3.16 eV higher than that of Ca^{+}: so Mg^{2+} ions are effective electron traps in CaO. The 5.7 eV emission is caused by a recombination of mobile holes with electrons trapped by magnesium ions. Similar to the 5.3 eV luminescence in a MgO crystal [25], the CaO emission band with a maximum at 4.63 eV has been attributed to the recombination of an electron with a hole trapped near a complex 'cation vacancy + defect (OH^{-} or Al^{3+})' [17]. Plastic strain of a CaO crystal leads to a sharp increase in the intensity of 2.8 eV emission, which is probably connected with the radiative annihilation of electronic excitations (EEs) near the association of anion and cation vacancies [26].

Using a double-vacuum monochromator the VUV luminescence of a freshly-cleaved CaO crystal was investigated during excitation by a 6 keV electron beam (the experimental set-up has been described in [26, 27]). A zero-phonon line at 5.88 eV has been detected on the short-wavelength edge of the above-mentioned 5.7 eV emission band [27]. A weak line

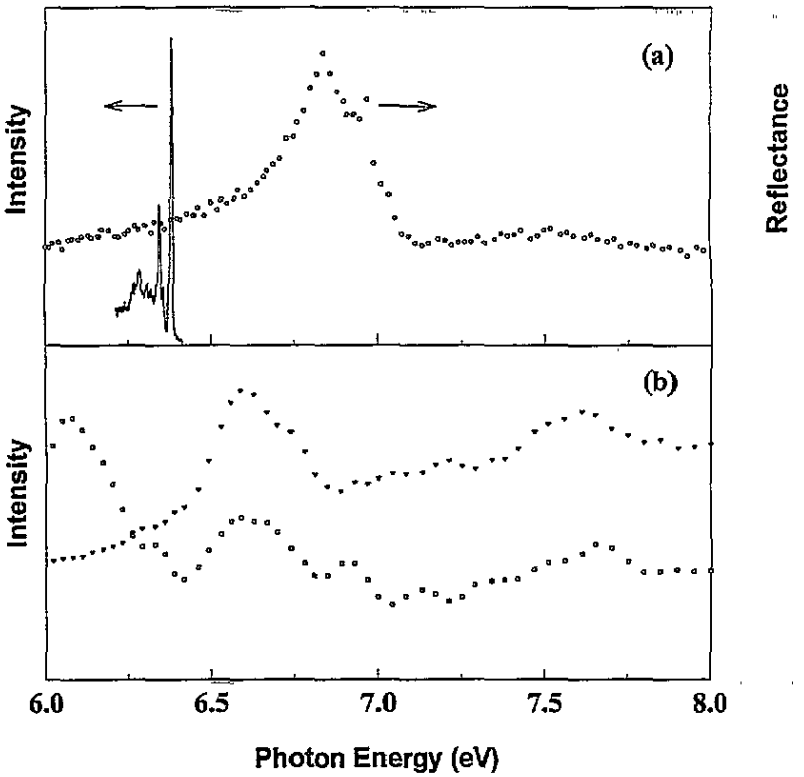

Figure 2. The reflection spectrum (○) (spectral resolution, 0.33 nm) and the excitation spectra (spectral resolution, 0.5 nm) of the 5.7 eV (□) and 4.63 eV (▽) emissions of a CaO crystal cleaved at LHeT in high vacuum. The spectrum of cathodoluminescence (——), of CaO was measured at 10 K.

at 6.38 eV with phonon side bands was observed in the short-wavelength region of the cathodoluminescence spectrum of CaO as well (figure 2(a)).

3.3. Excitation spectra of luminescence of a CaO crystal

We have measured for the first time the excitation spectra of 5.7, 4.63 and 2.8 eV emissions in a wide region of 6–32 eV for a CaO crystal cleaved at LHeT.

Figure 2(b) shows the excitation spectra of 5.7 and 4.63 eV emissions in the region of 6–8 eV. The 5.7 eV emission connected with the presence of magnesium ions has an excitation maximum at 6.07 eV, i.e. outside the region of the crystal's intrinsic absorption. The 4.63 eV emission can be effectively excited in the whole region of intrinsic absorption. It has a minimum near a broad reflection peak at 6.85 eV (see figures 1 and 2(a)) and maxima at 6.57 and 6.7 eV on the short-wavelength slope of intrinsic absorption. We have not yet succeeded in measuring the excitation spectrum of 6.38 eV emission. However, it should be noted that the position of this emission line probably coincides with the boundary of indirect band-to-band transitions.

Figure 3(b) presents the excitation spectra of 5.7, 4.63 and 2.8 eV emissions at LHeT in the region 6–32 eV. The intensity of all these emissions increases by more than twice when the energy of the exciting photons increases from 12 to 16.5 eV. The next intensity increase occurs at 21–24 eV. A significant decrease in the emission intensities is observed only for

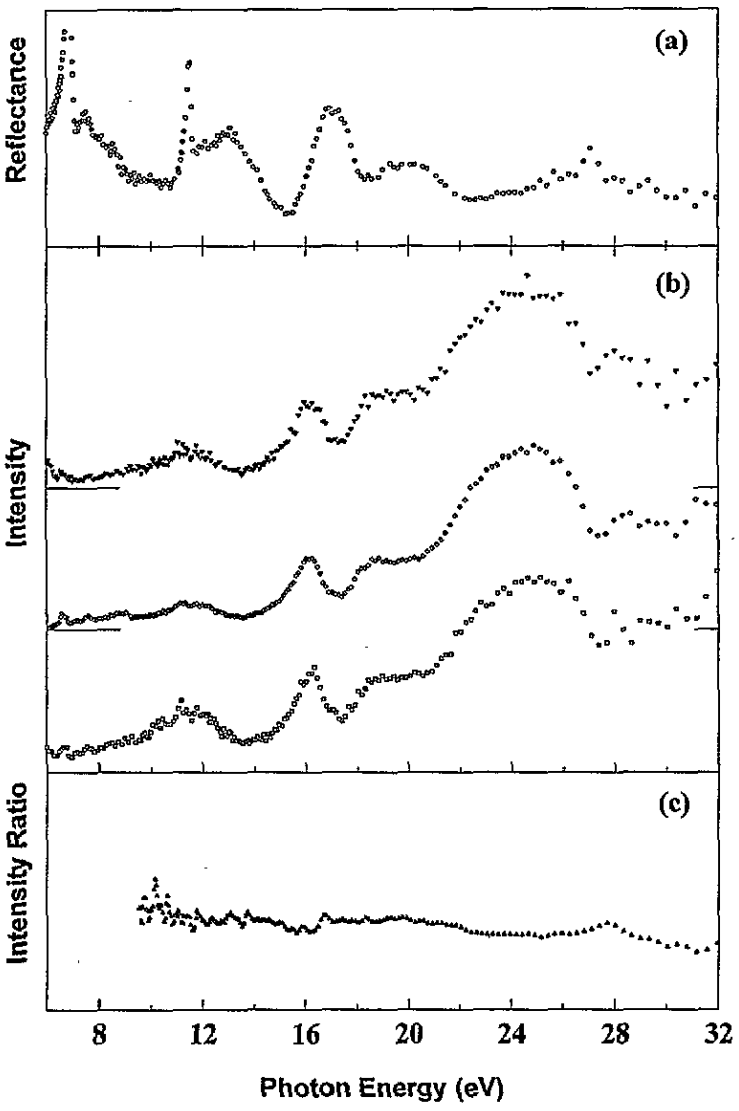

Figure 3. The reflection spectrum (○) and the excitation spectra of the 5.7 eV (▽), 4.63 eV (◇) and 2.8 eV (□) emissions and the intensity ratio spectrum for 5.7 and 4.63 eV emissions (△) measured at 8 K (spectral resolution, 0.25 nm) for a CaO crystal cleaved at LHeT in high vacuum.

$h\nu > 26$ eV. According to [15,28], excitation and ionization of cations start just in this energy region in CaO and CaS crystals. The excitation spectrum of UV luminescence has been measured at 80 K in a CaO:Be crystal [16]. The sharp increase in emission intensity at $h\nu > 15.5$ eV was there interpreted as a manifestation of the MEE process in CaO:Be. An analogous MEE process was also observed at $h\nu > 19.5$ eV in a MgO crystal [9, 29].

As in other ionic crystals, the changes in the emission intensities due to the variation in the exciting photon energy are partly connected with a selective reflection of SR by the crystal surface (no reflection correction was made in our excitation spectra) or with the non-radiative decay of mobile EEs at the surface. The probability of the latter process

increases for high absorption constants (i.e. in the region of intrinsic absorption of the crystal). However, a sharp increase in emission efficiency occurs in CaO in the region of 15–16.5 eV, where high absorption and reflection constants can lead only to a decrease in the emission intensity. Thus there is no doubt that the MEE process takes place in a CaO crystal.

Figure 3(c) shows the intensity ratio spectrum for 5.7 and 4.63 eV emissions at LHeT. As can be seen, this ratio is approximately constant between 10 and 32 eV.

3.4. Excitation spectra of luminescence for a $YAlO_3$ crystal

Broad reflection peaks (in comparison with the Γ exciton doublet in CaO) connected with the formation of excitons have been detected in Y_2O_3 and $YAlO_3$ crystals at 6 eV and 8 eV, respectively [7]. The reflection spectra as well as the spectra of optical constants have been measured in a wide spectral region up to 35 eV in Y_2O_3 and $YAlO_3$ [18, 30]. Broad luminescence with the maximum at 3.5 eV, caused by the radiative decay of STEs, can be excited in the region of intrinsic absorption of the crystal at 4–100 K in Y_2O_3 with an impurity content of a few parts per million [6]. The 5.9 eV emission (half-width, about 0.7 eV) can be excited in the long-wavelength region of intrinsic absorption of a $YAlO_3$ crystal at 80 K, whereas the photocreation of separated electrons and holes leads to the appearance of the 4.2 eV recombinational luminescence (half-width, about 0.9 eV) [18–20].

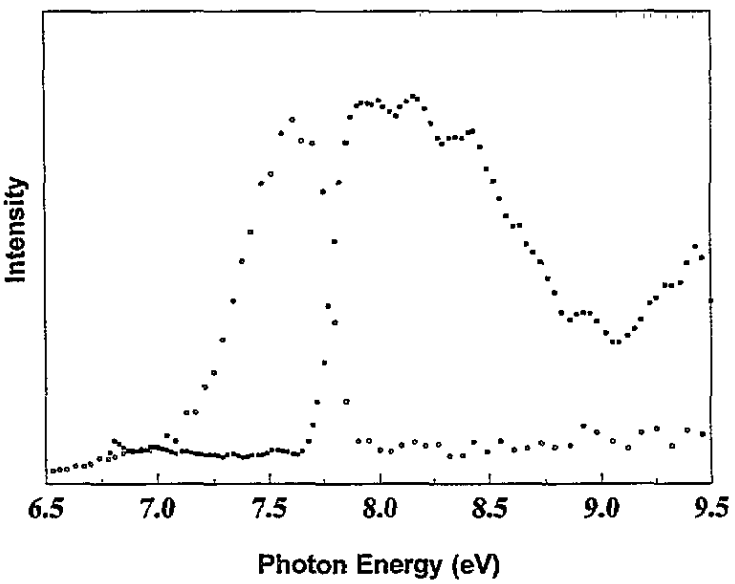

Figure 4. The excitation spectra of the 5.7 eV (■) and 4.35 eV (□) emissions of a $YAlO_3$ crystal measured at 8 K (spectral resolution, 0.33 nm).

Figures 4 and 5 show the excitation spectra of STE luminescence now obtained, for a $YAlO_3$ crystal at LHeT. A crystal face formed on the $YAlO_3$ growth was investigated. The excitation spectra of 5.87, 5.63 and 5.4 eV emissions, selected by a monochromator within the STE luminescence band, almost coincide. The efficiency of STE luminescence is high in the case of $YAlO_3$ excitation of photons of 7.7–8.7 eV, which selectively create excitons. In the short-wavelength spectral region the efficiency of the 5.9 eV emission decreases with

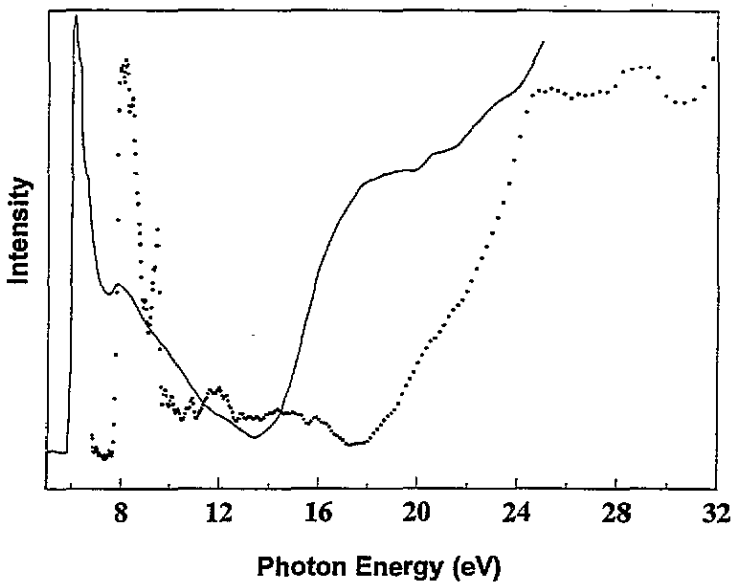

Figure 5. The excitation spectrum of 5.7 eV emission of a $YAlO_3$ crystal at 8 K (spectral resolution, 0.33 nm) (■). The excitation spectrum of the 3.5 eV emission of Y_2O_3 at 100 K (——) [11].

increase in the exciting photon energy and then sharply increases at $h\nu > 19$ eV. The excitation spectrum of STE emission (3.55 eV) in a Y_2O_3 crystal studied earlier by one of the present authors [11] is presented in figure 5 for comparison. The efficiency of STE emission in Y_2O_3 is high on the edge of the crystal's intrinsic absorption (6–7 eV), and low in the region of band-to-band transitions while it increases sharply at $h\nu > 14.5$ eV. According to our data the sharp increase in STE luminescence intensity in an Al_2O_3 crystal takes place at $h\nu > 23$ eV only.

To simplify the analysis of MEE processes in $YAlO_3$ we have studied the intensity ratio of the 5.9 and 4.2 eV emission bands at LHeT. The novel method of recording the intensity ratio of two different emissions belonging to the same crysal allowed us to eliminate effectively the influence of a selective reflection of SR by the crystal surface. The spectrum presented in figure 6 has a relatively simple shape; the value of the intensity ratio is approximately constant for 14–17 eV, increases sharply in the region of 17–20 eV and then decreases for 23–32 eV. This spectrum in a $YAlO_3$ differs considerably from the analogous ratio spectrum in a CaO crystal (compare with figure 3).

4. Discussion of experimental results

4.1. Possible mechanisms for the multiplication of electronic excitations in wide-gap crystals

The electron–hole MEE mechanism was revealed in silicon and germanium crystals by means of a photoelectric method (see, e.g., [31]). A photon with an energy exceeding the value of the threshold energy $E_{th}^{\pm} \simeq (3-4)E_g$ (E_g is the energy gap) creates a hot electron and a hot hole whose energies are sufficient for the formation of a secondary electron–hole pair. The spectra of recombinational luminescence excitation have been studied in wide-gap dielectrics

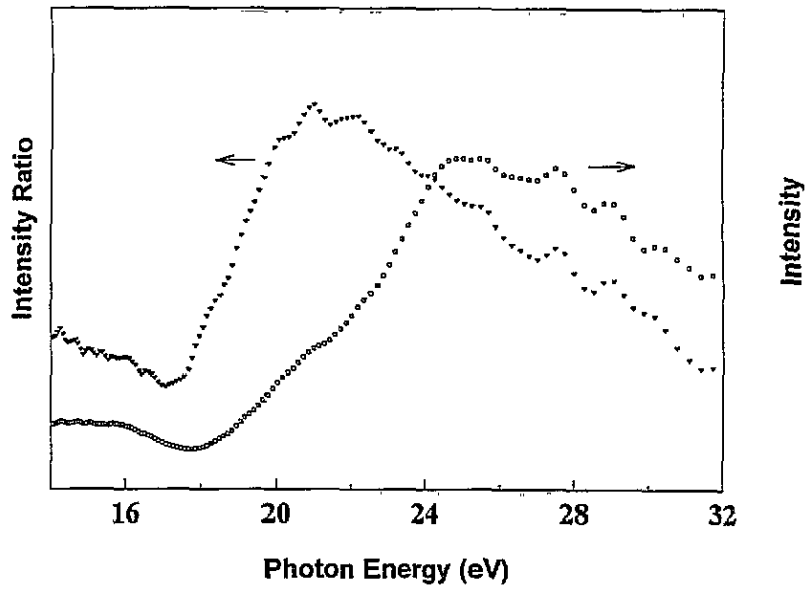

Figure 6. The excitation spectrum of the 4.3 eV emission (□) and the intensity ratio spectrum (▽) for 5.7 and 4.3 eV emissions measured at 8 K (spectral resolution, 0.33 nm) in a $YAlO_3$ crystal.

[32–34]. According to these investigations the electron–hole MEE mechanism has a high efficiency in ionic crystals as well. In all alkali halides and also in a MgO crystal the width of the valence band E_v is smaller than the value of E_g. In these systems, hot photoholes do not create new charge carriers and the MEE process is connected with the formation of secondary electon–hole pairs by hot photoelectrons. More strictly, this process can be interpreted as non-radiative Auger transtions between various branches in a conduction band with the formation of secondary electron–hole pairs (see, e.g., [34]).

The excitonic mechanism of MEE has been detected in alkali iodide crystals doped by luminescent impurity ions [32]. This mechanism which involves the creation of secondary excitons by hot photoelectrons has been quantitatively studied by the analysis of the spectrum of the intensity ratio of π to σ emissions of STEs on the excitation of a KBr crystal by SR at LHeT [35].

The third MEE mechanism connected with the decay of one cation EE with the formation of two anion EEs has been detected in KCl, RbCl, KBr and RbBr crystals (see, e.g., [22]). In these crystals the minimum ionization energy for cations is at least twice E_g.

4.2. Multiplication of electronic excitations in a CaO crystal

In a CaO crystal with narrow peaks in the short-wavelength region of intrinsic absorption the Γ excitons have relatively small oscillator strengths and an effective radius that significantly exceeds the interionic distance. The probability of the creation of excitons by electron impact is small in comparison with the probability of band-to-band transitions. As many theoretical calculations predict (see, e.g., the reviews in [36, 37]), the edge of intrinsic absorption in CaO is caused by indirect transitions from the Γ point of oxygen valence band to the X point of a conduction band formed mainly of d states.

The experimental data, mentioned in section 3.3, are in good agreement with these theoretical predictions. Indirect band-to-band transitions are repsonsible for the broad

reflection (absorption) band at 6.4–6.9 eV, i.e. at a lower energy than narrow reflection peaks connected with the Γ excitons (see figures 1 and 2(a)). The 4.63 eV luminescence connected with the recombination of electrons with holes localized near cation vacancies can effectively be excited in precisely this spectral region. It has been shown for a MgO crystal [25] that cation vacancies are not responsible for any selective absorption band beyond the region of the crystal's intrinsic absorption. The 5.7 eV luminescence connected with the recombination of holes with the electrons locallized on magnesium impurity ions has a main excitation band at 6–6.3 eV, i.e. out of the intrinsic absorption region as well. Similar to an AgBr crystal with indirect band-to-band transitions, the edge emission (6.38 eV) is observed at the edge of intrinsic absorption in a CaO crystal.

According to our experimental data the value of the energy gap for indirect $\Gamma \rightarrow X$ transitions is about 6.4 eV and the threshold energy of MEE in CaO, $E_{th}^{\pm} = 15.5$ eV, exceeds by 2.5 eV the $2E_g$. Part of the absorbed energy is transferred to a photohole, which is not able to form a secondary electron–hole pair ($E_v < E_g$ in CaO). In a simplified form the MEE theory for a system with two parabolic energy bands and effective mass m_e for electrons and effective mass m_h for holes results in a value of the threshold energy for the formation of a secondary electron–hole pair [33] given by

$$E_{th}^{\pm} = 2E_g\left(1 + \frac{m_e}{m_h}\right) \tag{1}$$

if the interaction with phonons is neglected; when the interaction with phonons is taken into account,

$$E_{th}^{\pm} = E_g\left(2 + \frac{m_e}{m_h}\right). \tag{2}$$

The values of $m_e/m_h = 0.21$ and $m_e/m_h = 0.42$ must be used in equations (1) and (2), respectively, in order to obtain the experimentally determined threshold energy for MEE in CaO (15.5 eV). The value of $m_e/m_h = 0.42$ is more reliable for a CaO crystal.

We have not succeeded in detecting the excitonic MEE mechanism in CaO. The intensity of the recombinational luminescence of CaO in the region of 22–24 eV (see figure 3(b)) increases owing to the generation of three anion EEs, on the average, by each absorbed photon. The excitation and ionization of cations take place in the region of 26–32 eV in CaO and CaS [15, 28]. We have observed peaks at 25–32 eV in the reflection spectrum of CaO at 8 K. The main peak in this region, at about 27 eV, is correlated with the sharp minimum in the spectrum of luminescence excitation (see figure 3). Similar to KCl and KBr [24, 34], the effective Auger decay of cation EEs with the formation of a double number of anion EEs takes place in CaO.

4.3. Multiplication of electronic excitations in a $YAlO_3$ crystal

In Y_2O_3, $YAlO_3$ and $Y_3Al_5O_{12}$ crystals, optically created excitons transform into a self-trapped state with a small effective radius. By analogy with alkali halides, the excitonic MEE mechanism as well as the electron–hole mechanism must occur in these crystals. An analysis of the spectrum of the intensity ratio for 5.9 and 4.2 eV (see figure 6) clearly demonstrates the formation of secondary excitons by hot photoelectrons. The threshold energy E_{th}^{0} of this process slightly exceeds 18 eV in $YAlO_3$ and is about 14 eV in Y_2O_3. The sharp increase in the 3.8 eV emission intensity in Al_2O_3 occurs at $h\nu > 23$ eV. These values of E_{th}^{0} exceed the value of $2E_g$ (approximately 13 eV, 17 eV and 19 eV for Y_2O_3, $YAlO_3$ and

Al_2O_3, respectively). In these crystals (as well as in CaO) with comparable values of m_e and m_h the energy excess of the absorbed photon is divided between a photoelectron and a photohole.

In a KBr crystal the ratio of STE π to σ emission intensities sharply increases with increase in the exciting photon energy and reaches a maximum value at an energy which is only 1 eV higher than E_{th}^0 [35]. When the data on electron impact spectroscopy for free atoms with singlet and triplet states is taken into account, this behaviour of the ratio function is typical for excitation of the triplet states. The spectrum of the intensity ratio for 5.9 and 4.4 eV in $YAlO_3$ has a sharp maximum at an energy of 2 eV higher than the value of the threshold energy. Apparently, the formation of secondary triplet excitons by hot photoelectrons takes place in a $YAlO_3$ crystal.

5. Conclusion

In a CaO crystal, where free excitons have large radii (in comparison with the lattice constant) and no self-trapping of excitons occurs in regular lattice sites, the electron–hole mechanism of the multiplication of charge carriers has been detected by means of luminescence methods. This MEE mechanism is also dominant in many other dielectrics and semiconductors with large-radius excitons (MgO, ZnO, ZnS, CdS, Si, Ge etc).

On the ther hand, the self-trapping of excitons takes place in $YAlO_3$ and the exciton radius is comparable with the lattice constant. Besides the universal electron–hole MEE mechanism, the excitonic mechanism conneced with the creation of secondary excitons by hot photoelectrons has been established in this system. The excitonic MEE mechanism is typical of other wide-gap ionic crystals with small-radius self-trapped excitons (Y_2O_3, NaCl, KCl, RbCl, CsCl, KBr, KI, etc).

Acknowledgments

This work has been supported by the Swedish Natural Science Research Council (NFR), the Royal Swedish Academy of Sciences, the Swedish Institute, the Crafoord Foundation, the Magnus Bergvall Foundation and the Carl Trygger Foundation.

References

[1] Abraham M M, Butler C T and Chen Y J 1971 *Chem. Phys.* **55** 3752
[2] Henderson B and Wertz J E 1977 *Defects in the Alkali Earth Oxides* (London: Taylor & Francis)
[3] Whited R C and Walker W C 1969 *Phys. Rev.* **188** 1380
[4] Lushchik Ch B, Kuusmann I L, Kuznetsov A I and Feldbach E H *Bull. Acad. Sci. USSR, Phys. Ser.* **52** 685
[5] Valbis Ya A, Kalder K A, Kuusmann I L, Lushchik Ch B, Rattas A A, Rachko Z A, Springis M E and Tiit V M 1975 *JETP Lett.* **22** 36
[6] Kuznetsov A I, Abramov V N, Roose N S and Savikhina T I 1978 *JETP Lett.* **28** 602
[7] Kuznetsov A I and Abramov V N 1978 *Sov. Phys.–Solid State* **20** 399
[8] Kuznetsov A I, Namozov B R and Mürk V V 1985 *Sov. Phys.–Solid State* **27** 1819
[9] Vasil'ev A N, Kolobanov V N, Kuusmann I L, Lushchik Ch B and Mikhailin V V 1985 *Sov. Phys.–Solid State* **27** 1616
[10] Aleksandrov Yu M, Lushchik Ch B, Makhov V N and Jakimenko M N 1985 *Bull. Acad. Sci. USSR, Phys. Ser.* **49** 1603
[11] Aleksandrov Yu M, Kuznetsov A I, Lushchik Ch B, Makhov V N, Meriloo I A, Savikhina T I, Syreishchikova T I and Jakimenko M N 1982 *Trudy Inst. Fiz. Akad. Nauk Estonskoi SSR* **53** 7

[12] Casabloni M and Grassano U M 1990 *J. Phys. Chem. Solids* **51** 805
[13] Maaroos A 1987 *Trudy Inst. Fiz. Akad. Nauk. Estonskoi SSR* **61** 126
[14] Whited R C and Walker W C 1969 *Phys. Rev. Lett.* **22** 1428
[15] Kaneko Y, Morimoto K and Koda T 1983 *J. Phys. Soc. Japan* **52** 4385
[16] Kolobanov B N, Lushchik Ch B, Maaroos A A, Mikhailin V V and Rogalev A L 1987 *Trudy Inst. Fiz. Akad. Nauk Estonskoi SSR* **61** 131
[17] Dolgov S, Kärner T, Maaroos A, Savikhina T and Vasil'chenko E 1994 *Phys. Status Solidi* b **186**
[18] Tomiki T, Kaminao M, Tanahara Y, Futemma T, Fujisawa M and Fukumode F 1991 *J. Phys. Soc. Japan* **60** 1799
[19] Kuznetsov A I, Abramov V N, Namozov B R and Uibo T V 1982 *Trudy Inst. Fiz. Akad. Nauk Estonskoi SSR* **52** 83
[20] Mürk V, Kuznetsov A, Namozov B and Ismailov K 1994 *Nucl. Instrum. Methods* B **91** 327
[21] Kink R, Lõhmus A, Niedrais H, Vaino P, Sorensen S, Huldt S and Martinson I 1991 *Phys. Scr.* **43** 517
[22] Kirm M, Martinson I, Lushchik A, Kalder K, Kink R, Lushchik Ch and Lõhmus A 1994 *Solid State Commun.* **90** 741
[23] Kuusmann I L and Lushchik Ch B 1976 *Bull. Acad. Sci. USSR, Phys. Ser.* **40** 14
[24] Boas J F, Clark M J and Pilbrow A 1976 *J. Phys. C: Solid State Phys.* **9** 4053
[25] Kalder K A, Kärner T N, Lushchik Ch B, Malycheva A F and Milenina R V 1976 *Soc. Phys.–Solid State* **40** 20
[26] Lushchik A, Feldbach E, Frorip A, Ibragimov K, Kuusmann I and Lushchik Ch 1994 *J. Phys.: Condens. Matter* **6** 2357
[27] Kuusmann I L, Liblik P H, Mugur R A, Tiit V M, Feldbach E H, Shatskina R V and Edula J J 1980 *Trudy Inst. Fiz. Akad. Nauk Estonskoi SSR* **51** 57
[28] Mikhailin V, Koch E E and Skibowski M 1974 *Vacuum Ultraviolet Radiation Physics* ed E E Koch, R Haensel and C Kunz (Oxford: Pergamon) p 401
[29] Gonzales R, Chen Y, Ballesteros C, Liu H, Williams G P, Rosenblatt G H, Williams R T and Gellerman W 1993 *Phys. Rev.* B **47** 4910
[30] Tomiki T, Tamashiro J, Tanahara Y, Yamada A, Fukutani H, Miyahara T, Kato H, Shin S and Ishigame M 1986 *J. Phys. Soc. Japan* **55** 4543
[31] Shockley W 1961 *Czech. J. Phys.* B **11** 8
[32] Ilmas E R, Kink R A, Liidya G G and Lushchik Ch B 1965 *Bull. Acad. Sci. USSR, Phys. Ser.* **29** 29
[33] Lushchik Ch B and Svaikhina T I 1981 *Bull. Acad. Sci. USSR, Phys. Ser* **45** 34
[34] Ilmas E R and Savikhina T I 1970 *J. Lumin.* **1–2** 702
[35] Lushchik A, Feldbach E, Lushchik Ch, Kirm M and Martinson I 1994 *Phys. Rev.* B **50**
[36] Lobatch V A, Rubin I R and Lushnikov P V 1990 *Phys. Status Solidi* b **161** 647
[37] Stepanyuk V S, Szasz A, Grigorenko A A, Katsnelson A A, Farberovich O V, Mikhailin V V and Hendry A 1992 *Phys. Status Solidi* b **173** 633